Hindawi
Advances in Polymer Technology
Volume 2023, Article ID 7640478, 9 pages
https://doi.org/10.1155/2023/7640478

Research Article

Studying the Fabrication and Characterization of Polymer Composites Reinforced with Waste Eggshell Powder

Wasan A. Alkaron,[1] **Sameer F. Hamad**,[2] **and Mohammed M. Sabri**[3]

[1]*Technical Institute of Basra, Southern Technical University, Basra, Iraq*
[2]*Department of Mechanical Engineering, University of Misan, Maysan 62001, Iraq*
[3]*Department of Physics, Faculty of Science and Health, Koya University, Koya, KOY45 Kurdistan Region, Iraq*

Correspondence should be addressed to Wasan A. Alkaron; w.alkaron@stu.edu.iq

Received 9 December 2022; Revised 16 March 2023; Accepted 20 March 2023; Published 29 March 2023

Academic Editor: Micaela Vannini

Polymeric and plastic materials currently have numerous positive impacts due to their unique properties that make them important for various engineering applications. However, sustainability is a vital factor that should be considered, because of environmental issues. Eggshells (ES) are an important way to reduce the impact of nondegradable materials when applied to reinforce different types of polymer matrices, whether natural or synthetic polymers. Therefore, this study is an attempt to explore the potential application of waste eggshell fillers for the first time as a natural reinforcement in polyamide 12 (PA) composites. PA was loaded with three different ratios (3, 5, and 10 wt. %) of eggshell powder. Morphological studies of the PA powder, ES powder, and their composites were carried out by scanning electron microscopy (SEM). Furthermore, differential scanning calorimetry (DSC) and Fourier transform infrared (FTIR) spectroscopy were performed to study the thermal and chemical properties of the raw materials and the produced composites. The results indicate ES fillers' potential usage as a reinforcement material to develop the thermal and chemical properties of the PA polymer matrix composites, thereby reducing costs and minimizing the environmental pollution caused by waste eggshells and petroleum-based polymers.

1. Introduction

Particle-reinforced polymer composites are attractive materials due to their moldability and their fabrication capability. The incorporation of rigid reinforcement particles into polymer matrices could enhance the properties of the produced composites, such as higher Young's modulus and strength [1]. Among thermoplastic polymer matrices, polyamide 12 (PA) is one of the most important applied matrices for polymer composites. Additionally, this material is a semicrystalline thermoplastic polymer and is considered a crucial material as a result of its economical production costs and its excellent chemical and thermal characteristics [2, 3]. Moreover, the PA12 polymer matrix presents excellent properties, such as low density, superior dimensional stability, and relatively higher flexural and tensile strengths [4, 5]. Furthermore, PA polymer composites have the ability to disseminate their applications with developed flame-retardant characteristics [2, 6]. Therefore, thermoplastic PA has been extensively used in different engineering applications, for example, in automotive, aircraft, aerospace, and in other industrial applications [3, 7]. However, due to sustainability problems and the worldwide environmental issues resulting from petroleum-based polymers, more attempts have been pursued to develop renewable and biodegradable resources [8, 9].

Eggshells (ES) are natural bioceramic composite materials, having a unique chemical composition that contains two main components. The first is about 95% of inorganic (calcium carbonate) and the second is 5% of organic, such as type X collagen and sulfated polysaccharides [8, 10, 11]. Therefore, these materials are mineral-rich and can be considered a source of Ca, one of the predominant ingredients [11, 12]. In contrast, several hundred metric tons of eggshell waste are produced annually worldwide by food industries. Consequently, the usage costs and the environmental effects of this waste are high [10, 11, 13, 14]. Such waste can be

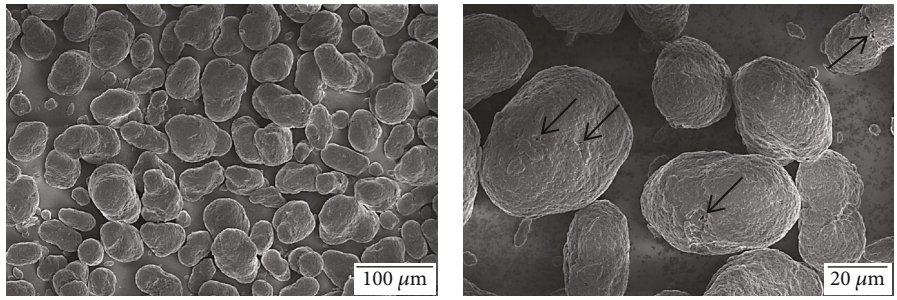

(a) (b)

Figure 1: SEM images of PA powder. (a) An overview and (b) detailed view of the surface morphology (arrows reveal micron-sized voids within particle).

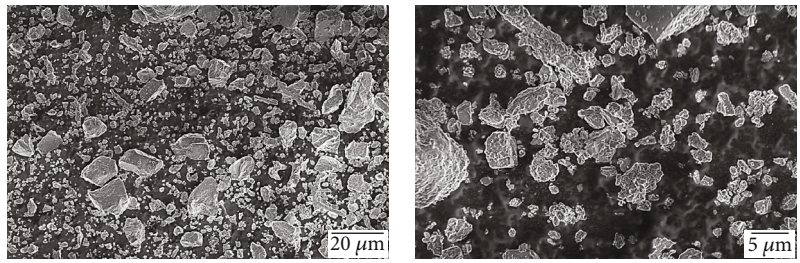

(a) (b)

Figure 2: SEM images of ES particles: (a) an overview and (b) detailed view of the surface morphology.

sustainably employed in inventive techniques via converting them to more valuable materials. The substantial availability of eggshells, combined with their characteristic structure, makes them a prospective source of bioreinforcement, which could be efficiently utilized for polymer composite materials. [8, 10, 15].

Based on the existing literature, several attempts have been made to reinforce different types of polymers using waste eggshell powder including, but not limited to, polypropylene [8, 16], high-density polyethylene [17, 18], and low-density polyethylene [14]. However, to our knowledge, none of the previous studies has dealt with reinforcing polyamide 12 matrix with waste eggshells. Thus, there is a need for such research to enhance the literature by utilizing waste eggshell as a bioreinforcement material with the expectation of improving the properties of PA composites.

Therefore, this research investigates and quantifies the impact of ES fillers on PA as a thermoplastic polymer matrix. For this purpose, thermoplastic PA composites were fabricated by using three different loading ratios of ES (3, 5, and 10 wt. %). Additionally, scanning electron microscopy (SEM) was utilized to investigate the surface morphology of the starting materials (ES and PA powders), as well as the distribution of the ES on the PA matrix. In addition, a morphological investigation of the fractured surface of the produced composites was undertaken using SEM. Moreover, thermal and chemical effects of the ES on the PA polymer matrix were investigated by DSC and FTIR spectroscopy, respectively. Thus, this study is an attempt to explore the potential application of waste eggshells, for the first time, as a natural reinforcement in PA composites.

Such a cheap and sustainable material as waste ES can definitely help in reducing costs and minimizing the environmental pollution caused by waste eggshells and petroleum-based polymers [19, 20]. Additionally, the implementation of these new biobased reinforcing materials into the structure of polyamide 12 matrix can broaden the scope of PA applications in various sectors, including industries that manufacture interior parts for automobiles, aircraft, and aerospace. The use of waste ES-reinforced PA composites offers improved properties at very low concentration which can meet the requirements of these industries by reducing weight and cost and increasing energy saving [14, 21].

2. Experimental Work

2.1. Materials. Thermoplastic Polyamide 12 (PA) powder (purchased from EOS (e-Manufacturing Solution)) was used as a polymer matrix. PA is a linearly synthesized polymer with repeating units linked together by amide bonds. The condensation reaction of amine and acid is the characteristic of PA formation [22]. The PA employed in this work was previously utilized in laser sintering, and to ensure the consistency for all samples, the same batch of powder was used for all prepared composites.

2.2. Preparation of Eggshell Powder. As a reinforcement material, fresh chicken eggs were bought from a market, and then the waste ES were initially washed and cleaned with tap water. Next, boiling water was used to remove any biological impurities stuck on the shells. Thereafter, the cleaned shells were dried at 50 °C for 12 hours using an electric oven. After that, the dried shells were broken by hand into small pieces before being ground to powder using a mixer, followed by the microsieving process.

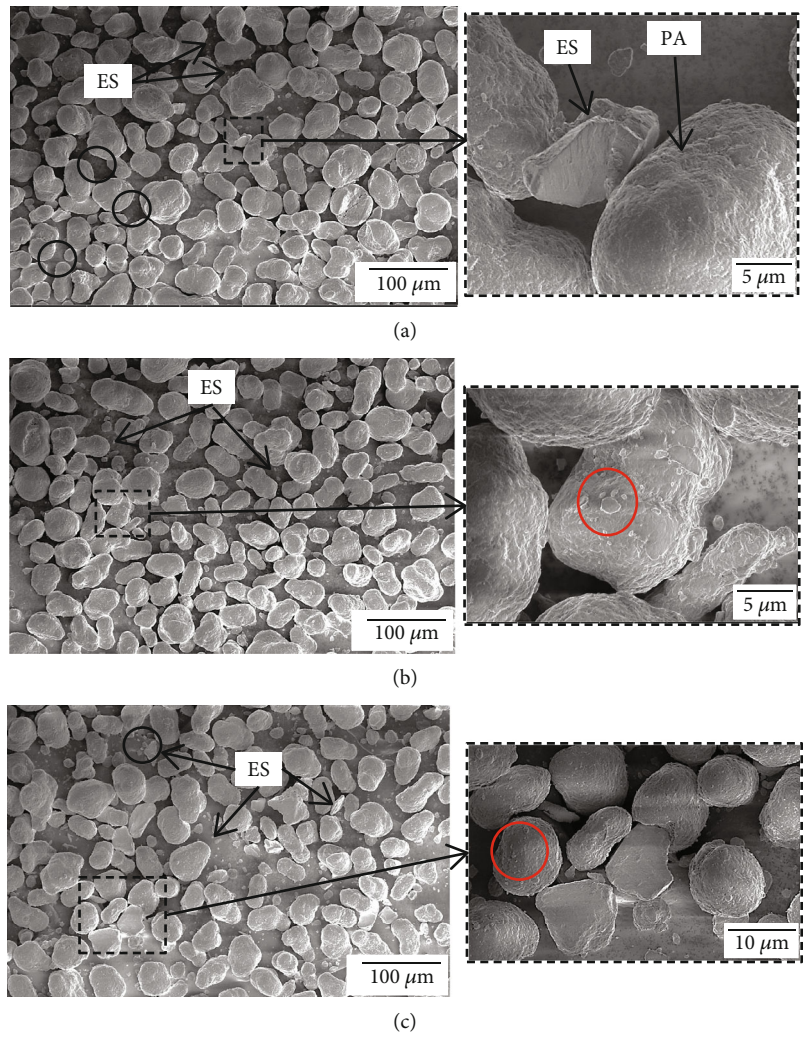

FIGURE 3: SEM images of PA/ES composite powders: (a) PA3 (the insert image shows the surface morphology of ES and PA particles); (b) PA5; and (c) PA10 (the insert image shows the physical interaction between ES and PA particles). Circles in (a) show less particle distribution of ES within the matrix. Circles in (c) show some agglomerated ES within the matrix. Circles in the insert micrographs of (b) and (c) show the fine ES were dispersed and distributed on the surface of a PA particle.

2.3. Production of Composites. PA powder was dry-mixed with ES powder in a small glass jar using a magnetic stirrer for one hour at a speed of 800 rounds per minute. Then, these glass jars containing the composite powders were transferred to an ultrasonic bath for another half an hour to improve the mixture's quality. To obtain solid samples, the produced composite powders were then put in a rectangular stainless mould (with dimensions of 20 mm wide × 80 mm long × 4 mm thick) and placed in an oven for 15 min at 200°C for curing. The content of ES fillers in the produced composites as mixed prior to curing was 3%, 5%, and 10% by weight. This will be referred to as PA3, PA5, and PA10, respectively.

2.4. Characterization

2.4.1. Scanning Electron Microscopy (SEM). The surface morphology of the PA powder and ES particles, as well as the produced composites and cross sections, were studied using the FEI Nova Nano SEM 450. The cured samples were cryofractured in the liquid nitrogen in order to observe the fractured surfaces. To obtain high-resolution images with low surface charging and avoid sample damage, a low accelerating voltage (1 kV) was applied with a working distance above 5 mm using an Everhart Thornley Detector (ETD) only.

2.4.2. Differential Scanning Calorimetry (DSC). Differential scanning calorimetry (DSC 4000 from Perkin Elmer) was used to study the thermal properties of the PA powder and its composite powders (PA3, PA5, and PA10). For each powder, 3 specimens were examined, and the average was taken. Then, 5 mg of powdered from each material was weighed and placed in a DSC-standard Al pan. Thereafter, each of these pans was punched and positioned in the DSC furnace. Then, each specimen was heated from about 25°C to 250°C with 10 K/min as a heating rate. Finally, the heating and cooling curves were obtained using the DSC-associated software of Pyris™.

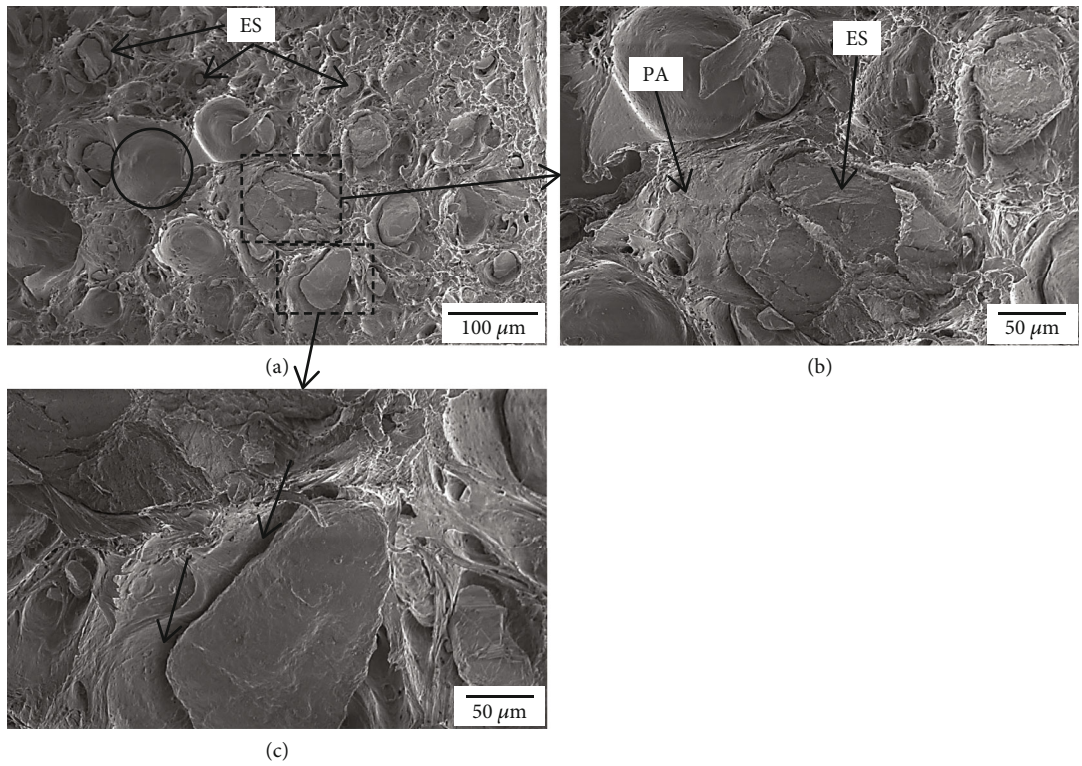

Figure 4: SEM images of the fractured surfaces of cured PA10 composites: (a) Overview of the fracture surface reveals the distribution of the ES particles in the PA matrix, (b) Reveals an embedded ES particle in the PA matrix, and (c) reveals de-bonded ES particle from the PA matrix. Circles in (a) show pull out particles (ES) from the matrix (PA). Arrows in (c) show a noticeable gap between the ES particle and PA matrix.

2.4.3. Fourier Transform Infrared (FTIR) Spectroscopy. The surface chemical compositions of the PA powder, ES powder, and their composite powders were investigated using a PerkinElmer Frontier spectrophotometer equipped with a Golden GateTM single reflection Diamond ATR accessory. The measurements were achieved without KBr dilution in the wavenumber range of 400 to 4000 cm^{-1}, with a record of 8 scans at a resolution of 2 cm^{-1}. Prior to collecting the spectra from the specimens, a background spectrum with no specimen was obtained as a control.

3. Results and Discussion

3.1. Surface Morphology of PA Powder and ES. The surface morphology of the PA powder (as received) was investigated using SEM, and the obtained micrographs are presented in Figure 1. An overview SEM micrograph of PA powder (Figure 1(a)) indicates the semispherical geometry or potato-shaped PA particles. Moreover, the size and morphology of these particles are extremely similar to each other, with only a small variation in their sizes ranging between 40 μm and 60 μm in diameter. However, similar SEM images (shape and geometry) of PA powder have been reported elsewhere [23, 24]. A higher magnification micrograph in this study (Figure 1(b)) shows that the surface of a PA particle is relatively rough with micron-sized voids on some particles (indicated by arrows). This could be attributed to the nature of the synthesis process.

The surface morphology of ES particles was also studied by SEM at two different magnifications, as shown in Figures 2(a) and 2(b). In Figure 2(a), most of the higher particles do not differ significantly from 20 micron (lower than 60 micron). This variation can be attributed to the nonhomogeneous grinding of the ES. The higher magnification SEM image (Figure 2(b)) indicates the rough surface and the irregular shape of these particles. This could be attributed to the highly brittle nature of eggshells [25].

3.2. Morphological Studies of PA/ES Composite Powders. An overview of SEM micrographs from the produced composite powders, with the three different loading ratios of ES fillers (PA3, PA5, and PA10), compared to the neat PA shown in Figures 1(a) and 1(b), is shown in Figures 3(a) and 3(c). From these images it can be confirmed that the process of producing composite powders does not affect/change the PA particles' geometry when compared with those particles before the mixing process (Figure 1(a)). Furthermore, SEM images (Figures 3(a) and 3(c)) reveal the ES particle (ESP) distribution in the PA powder. From Figure 3(a), it can be clearly seen that the ESPs are not uniformly dispersed in the matrix (less particle distribution within the matrix in some zones, indicated by circles in Figure 3(a)). This could be attributed to the low loading percentage of ES fillers that cannot cover all zones in the matrix. In addition, the insert micrograph in Figure 3(a) clearly reveals the surface morphology of both ES and PA particles.

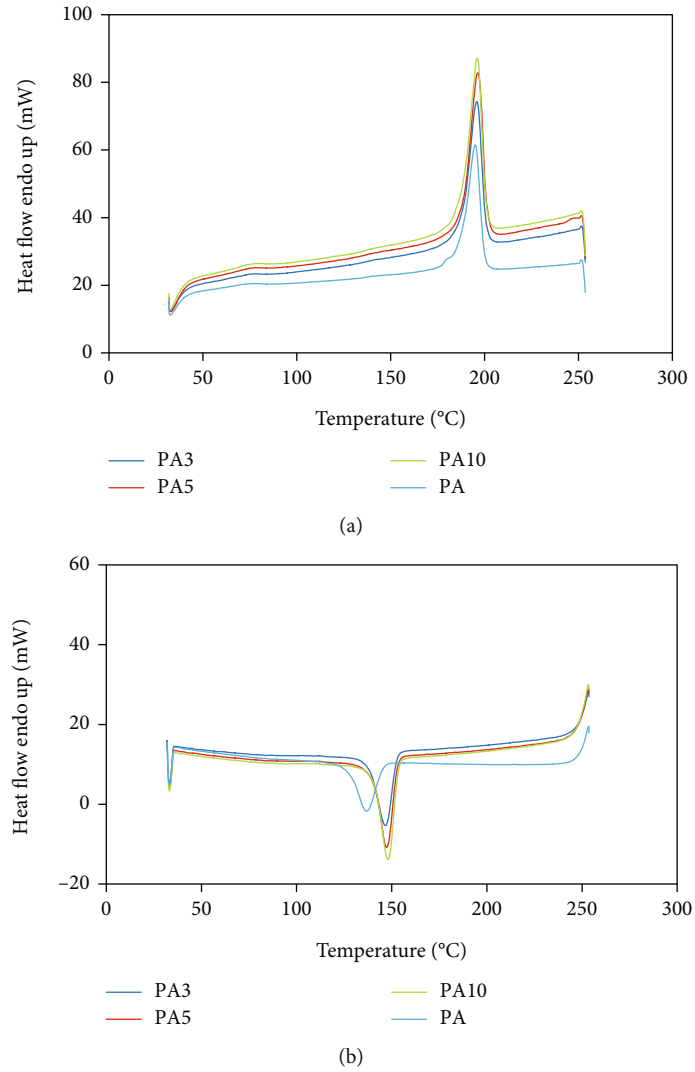

Figure 5: DSC results of PA and its composites (PA3, PA5, and PA10), showing (a) endothermic melting peak (peak up) and (b) exothermic cooling peak (peak down).

This could confirm the previous investigation (Figures 1 and 2) that the rough surface has the semispherical geometry of PA particles and the irregular shape of ES. Although large ES particles were seen at all loading ratios, the number of large ES particles in PA10 is higher than that in PA3 and PA5 (outlined by black circles in Figure 3(b)). Most notably, however, fine ES particles were well dispersed and distributed on the PA particle surfaces in PA5 and PA10 as can be observed by the inserts in Figures 3(b) and 3(c) (indicated by red circles).

Additionally, the insert micrograph (red circles Figure 3) reveals the physical interaction between two particles of PA and ES, which can significantly increase the thermal and mechanical properties.

3.3. Fractured Surfaces of ES/PA Composites. SEM images of the fractured surface of the PA10 composites are observed in Figure 4. The fracture surface presents ductile as well as brittle regions, with ES particles embedded and distributed within the matrix (Figure 4).

Moreover, the surface morphology of PA around the ES particles is relatively heterogonous, with rough, and porous surfaces. In addition, Figure 4(a) (indicated by circles) shows pull-out particles (ES) from the matrix (PA). This indicates the poor interfacial bonding between ES and PA. However, a higher magnification SEM image of the ES/PA interface (Figure 4(b)) reveals how the ES particle bonded and embedded within the PA matrix. Furthermore, Figure 4(c) shows the ES particle de-bonded and pulled out from the matrix with a noticeable gap between the ES and PA matrix (indicated by arrows). This variation in bonding between the ES and PA matrix could be attributed to the variations in the ES particles' surface morphology. There is good interlocking and well-embedded ES in the PA matrix when the ES particles' surface morphology is relatively rough, while the poor interfacial bonding between ES and the PA matrix could occurred when the surface morphology of ES the particle is relatively smooth.

3.4. Thermal Investigations by DSC. The distinct influence of particles as a reinforcement material on the crystalline

Table 1: Thermal properties of PA and its composites (PA3, PA5, and PA10).

Property/sample	PA		PA3		PA5		PA10	
	Measured	Stad. error	Measured	Stad. error	Measured	Stad. error	Measured	Stad. error
T_m (c)	195	0.05	195.8	0.48	196.47	0.85	196.08	0.54
$\triangle H_m$ (J/g)	93.94	1.53	82.93	1.43	92.27	1.07	80.06	1.91
T_c (c)	136.8	0.50	146.7	0.59	147.4	0.70	148.0	1.21
$\triangle H_c$ (J/g)	39.92	1.29	39.99	1.85	41.87	1.50	38.51	1.37
X_c (%) (calculated from Equation (1))	44.64		39.98		45.37		39.60	

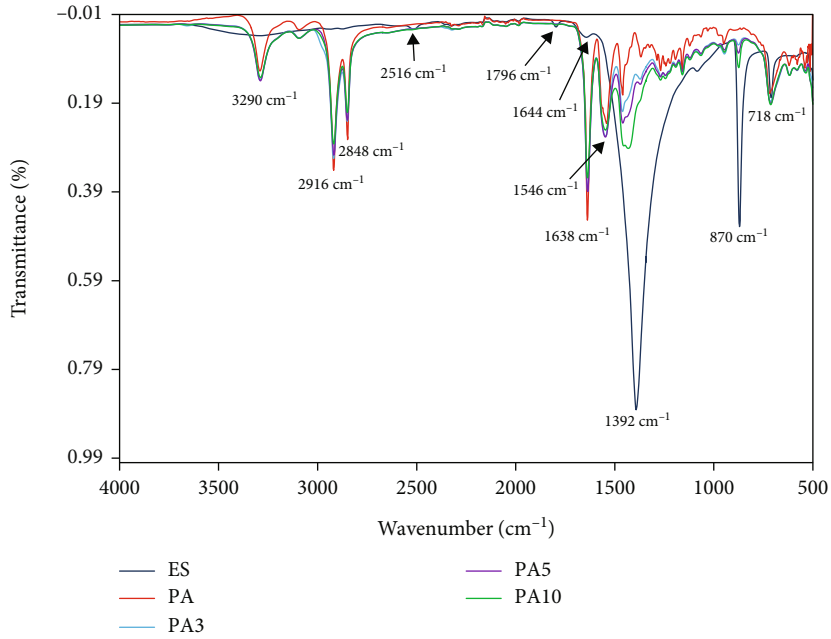

Figure 6: Fourier transform infrared (FTIR) spectra of PA and ES as well as ESPs/PA12 composites (PA3, PA5, and PA10).

structure of semicrystalline polymers is their capability to act as a nucleating agent [15, 26]. The thermal behavior of PA and ES/PA composites was estimated by DSC. The DSC heating and cooling thermograms of PA matrix and its composites (3, 5, and 10 wt. % of ES) are shown in Figure 5. Furthermore, Table 1 presents the thermal properties of ES/PA composites, including the melting temperature (T_m), crystallization temperature (T_c), enthalpy of crystallization ($\triangle H_c$), and enthalpy of melting ($\triangle H_m$). The degree of crystallinity (X_c) of PA and composites was calculated using the following equation [27]:

$$Xc = \frac{\triangle Hm}{\left(1 - \phi_f\right)\triangle H0} * 100, \quad (1)$$

where $\triangle H_m$ is the heat of melting of the sample (J/g), and $\triangle H_o$ represents the heat of fusion value for a theoretically 100% crystalline PA (209.3 J/g) [28], while ϕ_f is the ES weight fraction.

The results in Table 1 show an increase in melting temperature (T_m), which could indicate a reduction in the flexibility of chains [26, 29]. The enthalpy of melting ($\triangle H_m$) of PA matrix was higher than that of ES/PA composites, thereby demonstrating the substitution effect of some PA by ES [26]. Moreover, values in Table 1 show an increase in crystalline temperature (T_c), which is of 7% after the addition of 5 and 10 wt. % of ES (the increase is lower than 0.5% in each case). Moreover, the crystallinity percentage (X_c) of PA was also affected by the incorporation of ES. As can be seen in Table 1, with the addition of 3 wt. % of ES (PA3) to the PA matrix, the crystallinity percentage changed slightly. However, an increase in the degree of crystallinity is observed with the addition of 5 wt. % ES (PA5). It has been reported that calcium carbonate present in eggshells promotes and enhances polymer crystallinity [15, 26]. In contrast, the degree of crystallinity decreased slightly when adding 10 wt. % of ES (PA10), in comparison with that of PA5. This influence contributed to a better diffusion of particles in the PA12 matrix when the loading ratio of ES was 5 wt. % (PA5).

3.5. Chemical Analysis by FTIR. To further understand the actual interaction between ES and PA in the PA/ES composites, FTIR absorption spectra were collected. Figure 6 shows the collected FTIR spectra of PA powder and ES powder, as well as PA/ES composites (PA3, PA5, and PA10). The observed band positions in the FTIR spectra of the PA1 and PA/ES composites and their assignments are in a good

agreement with previous studies [30–33]. From Figure 6, it is clear that PA shows a peak at a wave number of 3290 cm^{-1}, related to hydrogen-bonded N-H stretching. The other observed adjacent peaks at around 2916 and 2848 cm^{-1} are assigned to the methylene asymmetric and symmetric stretching vibrations. The characteristic vibration at 1638 cm^{-1} is due to C=O carbonyl group, while the wavenumber region at 1546 cm^{-1} is attributed to the secondary amides (-CN and –NH deformation) [32]. The band at about 1460 cm^{-1} is due to primary amides (C-CO-NH_2) [32]. The obtained peaks at 950 and 1160 cm^{-1}, belong to the crystalline and amorphous regions, respectively [32]. The absorption bands at about 718 and 620 cm^{-1} are related to the primary amides N-H and C=O out of plane bending, respectively [30, 32].

The FTIR spectrum of ES in Figure 6 revealed two absorption bands at 710 and 870 cm^{-1}. The existence of these two bands in the FTIR spectra indicates the existence of calcium carbonate ($CaCO_3$) [34, 35]. Furthermore, the observed strong peak at around 1392 cm^{-1} is attributed to the existence of carbonate minerals of the eggshell structure [34]. The peak observed at 2516 cm^{-1} may be assigned to the presence of a hydrogen group (-OH) stretching in the eggshell structure [34, 36]. The observed peaks at 1644 and 1796 cm^{-1} resulted from the carbonyl group (C=O) stretching presented in the ES structure [34].

However, the FTIR spectra of the ES/PA composites (Figure 6) indicated an absorption peak at a wavenumber of 870 cm^{-1}. This band was clearly seen in the FTIR spectra of ES, whereas there was no absorption peak in this wavenumber range in the PA spectra. This absorption band in the spectra of ES was attributed to the existence of calcium carbonate ($CaCO_3$) in the ES structure [34, 35]. Therefore, the observed peak in the spectra of ES/PA composites can be attributed to the chemical interaction between PA and $CaCO_3$ presented in the ES structure. Moreover, the intensity of this peak was observed to gradually increase as the loading ratio of ES increased in the ES/PA system. This indicates increased incorporation of $CaCO_3$ within the PA matrix composites.

Although this article does not consider the mechanical properties in the experimental methodology, the results obtained show an improvement in the thermal-chemical properties of the resultant composites that can positively affect their mechanical properties. Previous studies have shown similar findings in that the mechanical properties can be improved alongside good dispersion of the filling materials and an improvement in the thermal properties [8, 19, 21].

4. Conclusions

In this present work, the ES/PA composites with three different loading ratios of ES fillers (3, 5, and 10 wt. %) were fabricated. The morphological analysis of the starting materials and the interfacial morphology of the produced composites have been explored using SEM. Furthermore, the thermal and chemical properties of the ES and PA powders together with their composites have been studied by DSC and FTIR, respectively. The outcome of the characterization of ES/PA composites suggests that a composite with 5 wt. % of ES (PA5) has the potential for better ES particle distribution. The observations obtained by SEM demonstrated that the ES particles were relatively uniformly dispersed in the matrix at 5 wt. %, and better than at 10 wt. %, due to the agglomeration of ES particles between PA particles. This finding interprets the results obtained for the DSC as the best results of thermal properties having been obtained at 5 wt. %. The reason for that is that the surface morphology of the ES particles can significantly affect the interfacial bonding between the ES and PA matrix. The ES affect the thermal properties of the polymer matrix, and thus the crystallinity and crystallization temperature were substantially influenced by the presence of the ES, as shown by the DSC results. Furthermore, FTIR studies show interaction between $CaCO_3$ presented in the ES structure and PA matrix. Therefore, the results obtained in this work provide a better understanding of the incorporation of ES in the system of ES/PA composites, thus indicating the potential usefulness of waste ES as a reinforcement for polymer composites. According to the summarized results, the ES can be easily and efficiently used as reinforcement materials to replace the other filling materials that use harmful substituents like organoclay. Although these are encouraging results, future work could include the tensile properties to directly investigate the effects of ES on the strength, elongation, and elastic modulus of the resultant composite.

Data Availability

The authors confirm that the raw data which support the findings and results of this study are available from the corresponding author, upon reasonable request.

Disclosure

This research was performed as part of the employment of the authors. The employers of the authors are Wasan A. Alkaron (Southern Technical University), Sameer H. Fahad (University of Misan), and Mohammed M. Sabri (Koya University).

Conflicts of Interest

The authors declare that there is no conflict of interest regarding the publication of this article.

References

[1] G. Narendar and V. C. Sekhar, "Preparation and testing of composites with slag and egg shell powder filler," *International journal of Engineering Research and Applications*, vol. 8, no. 6, pp. 57–60, 2018.

[2] A. Öztürk, F. Saribal, Ş. Duman, M. Akkoyun, Ş. E. N. Ibrahim, and D. Ovali, "Polyamide 12/antimony trioxide/sepiolite or boron composites: mechanical properties and flame retardancy," *Çukurova University, Journal of Faculty of Engineering and Architecture*, vol. 35, no. 4, pp. 1083–1090, 2020.

[3] A. Borić, A. Kalendová, M. Urbanek, and T. Pepelnjak, "Characterisation of polyamide (PA)12 nanocomposites with montmorillonite (MMT) filler clay used for the incremental forming of sheets," *Polymers (Basel)*, vol. 11, no. 8, p. 1248, 2019.

[4] A. Kausar, "Advances in carbon fiber reinforced polyamide-based composite materials," *Advances in Materials Science*, vol. 19, no. 4, pp. 67–82, 2019.

[5] T. Dhanavendhan, P. Elavarasan, R. Jeevanantham, and S. C. Prasanna, "Investigation on the mechanical properties of natural fibers reinforced with egg shell," *International Journal of Engineering Research & Technology*, vol. 3, no. 3, pp. 177–180, 2017.

[6] T. Glaskova-Kuzmina, D. Dejus, J. Jātnieks et al., "Flame-retardant and tensile properties of polyamide 12 processed by selective laser sintering," *Journal of Composites Science*, vol. 6, no. 7, p. 185, 2022.

[7] B. Guo, Z. Xu, X. Luo, and J. Bai, "A detailed evaluation of surface, thermal, and flammable properties of polyamide 12/glass beads composites fabricated by multi jet fusion," *Virtual and Physical Prototyping*, vol. 16, no. sup1, pp. S39–S52, 2021.

[8] Y. Feng, B. Ashok, K. Madhukar et al., "Preparation and characterization of polypropylene carbonate bio-filler (eggshell powder) composite films," *International Journal of Polymer Analysis and Characterization*, vol. 19, no. 7, pp. 637–647, 2014.

[9] R. Kishore, G. Karthick, M. D. Vijayakumar, and V. Dhinakaran, "Analysis of mechanical behaviour of natural filler and fiber based composite materials," *International Journal of Recent Technology and Engineering*, vol. 8, no. 1, pp. 117–121, 2019.

[10] S. B. Hassan, V. S. Aigbodion, and S. N. Patrick, "Development of polyester/eggshell particulate composites," *Tribology in Industry*, vol. 34, no. 4, pp. 217–225, 2012.

[11] I. O. Oladele, B. A. Makinde-Isola, A. A. Adediran, M. O. Oladejo, A. F. Owa, and T. M. A. Olayanju, "Mechanical and wear behaviour of pulverised poultry eggshell/sisal fiber hybrid reinforced epoxy composites," *Materials Research Express*, vol. 7, no. 4, 2020.

[12] J. Senthil and R. P. Madan, "Preparation and characterization of reinforced egg shell polymer composites," *International Journal on Mechanical Engineering and Robotics*, vol. 3, no. 3, pp. 7–17, 2015.

[13] D. Nath, K. Jangid, A. Susaniya, R. Kumar, and R. Vaish, "Eggshell derived CaO-Portland cement antibacterial composites," *Composites Part C: Open Access*, vol. 5, p. 100123, 2021.

[14] S. A. Bello, N. K. Raji, M. Y. Kolawole et al., "Eggshell nanoparticle reinforced recycled low-density polyethylene: a new material for automobile application," *Journal of King Saud University - Engineering Sciences*, 2021.

[15] D. S. Villarreal-Lucio, J. L. Rivera-Armenta, A. L. Martinez-Hernandez, and I. A. Estrada-Moreno, "Effect of eggshell particle size in thermal and thermomechanical properties of PP/eggshell composites," *International Journal of Engineering Research & Technology*, vol. 7, no. 8, pp. 305–313, 2018.

[16] A. A. Younis and A. A. El-Wakil, "New composites from waste polypropylene/eggshell characterized by high flame retardant and mechanical properties," *Fibers and Polymers*, vol. 22, no. 12, pp. 3456–3468, 2021.

[17] R. Dweiri, "Processing and characterization of surface treated chicken eggshell and calcium carbonate particles filled high-density polyethylene composites," *Materials Research*, vol. 24, no. 3, 2021.

[18] M. Sharmeeni, M. Yamuna, M. Mathialagan, and I. Hanafi, "Development of HDPE-modified eggshell composite," *Polymer Composites*, vol. 39, pp. 1630–1637, 2016.

[19] N. H. Ononiwu, C. G. Ozoegwu, N. Madushele, and E. T. Akinlabi, "Carbonization temperature and its effect on the mechanical properties, wear and corrosion resistance of aluminum reinforced with eggshell," *Journal of Composites Science*, vol. 5, no. 10, p. 262, 2021.

[20] S. Owuamanam and D. Cree, "Progress of bio-calcium carbonate waste eggshell and seashell fillers in polymer composites: a review," *Journal of Composites Science*, vol. 4, no. 2, p. 70, 2020.

[21] A. Rahman, M. A. Chowdhury, M. B. A. Shuvho, N. Hossain, M. Fotouhi, and R. Ali, "Fabrication and characterization of jute/cotton bio-composites reinforced with eggshell particles," *Polymer Bulletin*, vol. 80, no. 1, pp. 931–957, 2022.

[22] L. Verbelen, S. Dadbakhsh, M. Van Den Eynde, J. P. Kruth, B. Goderis, and P. Van Puyvelde, "Characterization of polyamide powders for determination of laser sintering processability," *European Polymer Journal*, vol. 75, pp. 163–174, 2016.

[23] L. Lanzl, K. Wudy, S. Greiner, and D. Drummer, "Selective laser sintering of copper filled polyamide 12: characterization of powder properties and process behavior," *Polymer Composites*, vol. 40, no. 5, pp. 1801–1809, 2019.

[24] B. Chen, R. Davies, Y. Liu et al., "Laser sintering of graphene nanoplatelets encapsulated polyamide powders," *Additive Manufacturing*, vol. 35, p. 101363, 2020.

[25] G. Ramesh, D. Jayabalakrishnan, and C. Rameshkumar, "Mechanical and thermal characterization of heat/surface treated egg shell filler diffused natural rubber green composite," *Journal of Optoelectronics and Biomedical Materials*, vol. 10, no. 1, pp. 21–28, 2019.

[26] A. Praditttham, N. Charitngam, S. Puttajan, D. Atong, and C. Pechyen, "Surface modified CaCO3 by palmitic acid as nucleating agents for polypropylene film: mechanical, thermal and physical properties," *Energy Procedia*, vol. 56, pp. 264–273, 2014.

[27] B. Van Hooreweder, D. Moens, R. Boonen, J. P. Kruth, and P. Sas, "On the difference in material structure and fatigue properties of nylon specimens produced by injection molding and selective laser sintering," *Polymer Testing*, vol. 32, no. 5, pp. 972–981, 2013.

[28] G. Craft, J. Nussbaum, N. Crane, and J. P. Harmon, "Impact of extended sintering times on mechanical properties in PA-12 parts produced by powderbed fusion processes," *Additive Manufacturing*, vol. 22, pp. 800–806, 2018.

[29] A. Buasri, N. Chaiyut, K. Borvornchettanuwat, N. Chantanachai, and K. Thonglor, "Thermal and mechanical properties of modified CaCO 3 / PP nanocomposites," *International Journal of Materials and Metallurgical Engineering*, vol. 6, no. 8, pp. 446–449, 2012.

[30] N. Ma, W. Liu, L. Ma et al., "Crystal transition and thermal behavior of nylon 12," *E-Polymers*, vol. 20, no. 1, pp. 346–352, 2020.

[31] G. Prasad, R. P. S. Chakradhar, P. Bera, A. A. Prabu, and C. Anandan, "Transparent hydrophobic and superhydrophobic coatings fabricated using polyamide 12–SiO2 nanocomposite," *Surface and Interface Analysis*, vol. 49, no. 5, pp. 427–433, 2017.

[32] B. M. de Campos, P. S. Calefi, K. J. Ciuffi et al., "Coating of polyamide 12 by sol-gel methodology," *Journal of Thermal Analysis and Calorimetry*, vol. 115, no. 2, pp. 1029–1035, 2014.

[33] R. Kuracina, Z. Szabová, E. Buranská, A. Pastierová, P. Gogola, and I. Buranský, "Determination of fire parameters of polyamide 12 powder for additive technologies," *Polymers (Basel)*, vol. 13, no. 17, p. 3014, 2021.

[34] M. S. Tizo, L. A. V. Blanco, A. C. Q. Cagas et al., "Efficiency of calcium carbonate from eggshells as an adsorbent for cadmium removal in aqueous solution," *Sustainable Environment Research*, vol. 28, no. 6, pp. 326–332, 2018.

[35] O. Awogbemi, F. Inambao, and E. I. Onuh, "Modification and characterization of chicken eggshell for possible catalytic applications," *Heliyon*, vol. 6, no. 10, p. e05283, 2020.

[36] M. Ahmad, A. R. A. Usman, S. S. Lee et al., "Eggshell and coral wastes as low cost sorbents for the removal of Pb^{2+}, Cd^{2+} and Cu^{2+} from aqueous solutions," *Journal of Industrial and Engineering Chemistry*, vol. 18, no. 1, pp. 198–204, 2012.